ORIGINAL ARTICLE

Structural and functional changes of PSI-LHCI supercomplexes of *Chlamydomonas reinhardtii* cells grown under high salt conditions

Rajagopal Subramanyam · Craig Jolley · Balakumar Thangaraj · Sreedhar Nellaepalli · Andrew N. Webber · Petra Fromme

Abstract The effect of high salt concentration (100 mM NaCl) on the organization of photosystem I-light harvesting complex I supercomplexes (PSI-LHCI) of *Chlamydomonas reinhardtii* was studied. The electron transfer activity was reduced by 39% in isolated PSI-LHCI supercomplexes. The visible circular dichroism (CD) spectra associated with strongly coupled chlorophyll (Chl) dimers were reduced in intensity, indicating that pigment–pigment interactions were disrupted. This data is consistent with results from fluorescence streak camera spectroscopy, which suggest that red-shifted pigments in the PSI-LHCI antenna had been lost. Denaturing gel electrophoresis and immunoblot analysis reveals that levels of the PSI reaction center proteins PsaD, PsaE and PsaF were reduced due to salt stress.

PsaE is almost completely absent under high salt conditions. It is known that the membrane-extrinsic subunits PsaD and E form the ferredoxin-docking site. Our results indicate that the PSI-LHCI supercomplex is damaged by reactive oxygen species at high salt concentration, with particular impact on the ferredoxin-docking site and the PSI-LHCI interface.

Abbreviations

CD	Circular dichroism
Chl	Chlorophyll
DDM	*n*-Dodecyl-β-maltoside
LHC	Light harvesting complex
MALDI-TOF	Matrix assisted laser desorption ionization time-of-flight mass spectrometry
PS	Photosystem
SOD	Superoxide dismutase

R. Subramanyam (✉) · S. Nellaepalli
Department of Biochemistry, School of Life Sciences,
University of Hyderabad, Hyderabad 500046, India
e-mail: srgsl@uohyd.ernet.in

R. Subramanyam · A. N. Webber
The Center for Bioenergy and Photosynthesis,
School of Life Sciences, Arizona State University,
PO Box 874501, Tempe, AZ 85287, USA

R. Subramanyam · B. Thangaraj · P. Fromme
Department of Chemistry and Biochemistry,
The Center for Bioenergy and Photosynthesis,
Arizona State University, Tempe, AZ 85287-1604, USA

C. Jolley
Department of Physics,
The Center for Bioenergy and Photosynthesis,
Arizona State University, Tempe, AZ 85287-1504, USA

Present Address:
C. Jolley
Department of Chemistry and Biochemistry,
Montana State University, Bozeman, MT 59717, USA

Introduction

Salinity-stress effects on plant growth often involve impairment of photosynthesis. High amounts of sodium in the soil impair cell metabolism and photosynthesis by increasing osmotic pressure (Brini et al. 2007). The molecular mechanisms responsible for the salt-induced inactivation of the photosynthetic machinery have been studied extensively, with particular focus on photosystem II (PSII), in vitro (Miyao and Murata 1983) and in vivo (Allakhverdiev et al. 1999, 2000; Demetriou et al. 2007). When PSII membrane

fragments are exposed to high concentrations of NaCl, the extrinsic proteins of the oxygen-evolving machinery of PSII dissociate from the membrane-intrinsic complex, resulting in impairment of oxygen evolution (Murata and Miyao 1985). In cyanobacterial cells, high concentrations of NaCl also inactivate Na^+/H^+ antiporters (Allakhverdiev et al. 1999, 2000).

Exposure of the green alga *Dunaliella tertiolecta* to salinity stress results in a significant inhibition of photosynthesis, due to a decrease in PSII activity (Gilmour et al. 1985). A decrease in PSII activity has also been associated with the transition to State 2. This was confirmed by Endo et al. (1995), who also suggested a connection between the decrease in PSII quantum yield caused by salinity stress and that caused by state transitions in *Chlamydomonas reinhardtii*. In the red alga *Porphyra perforata*, Satoh et al. (1983) demonstrated that the salinity stress-induced decrease in PSII activity was due to a decrease in the excitation energy reaching PSII reaction centers, as well as damage to the oxidizing side of PSII. Salt stress also inhibits PSII activity in higher plants (Everard et al. 1994; Tiwari et al. 1997; Misra et al. 1999), including salt-tolerant plants such as mangroves (Parida et al. 2003). In some reports, the effects of salt stress on PSII were due to the dissociation of the 23-kDa polypeptide extrinsically bound to PSII (Murata et al. 1992). Salt stress has also been reported to reduce D_1 protein turnover in both cyanobacteria and plants (Al-Taweel et al. 2007; Allakhverdiev and Murata 2008).

The mechanism of salt stress has also been well established in cyanobacteria (Verma and Mohanty 2000a, b; Lu and Vonshak 2002; Sudhir et al. 2005). It leads to electron transport inhibition at both the donor and the acceptor sides of PSII, damage to the phycobilisomes (membrane-extrinsic antenna of PSII) as reflected by a significant decrease in phycocyanin content, and a shift in the distribution of excitation energy from PSII to PSI as suggested by an increase in qN (Verma and Mohanty 2000a, b; Lu and Vonshak 2002; Sudhir et al. 2005). In a study using the cyanobacterium *Spirulina*, the downregulation of PSII reaction center proteins was observed without any inhibition of electron transfer on the donor and acceptor sides of PSII (Lu and Vonshak 1999), suggesting that the effects of salt stress on PSII may vary between species. A very recent paper by Gong et al. (2008) reports that there were no significant changes in the levels of the CP47, CP43, cytochrome c550, and D1 proteins. The PsbO content in isolated thylakoids, however, decreased. Recent reports show that the effects of salt stress on higher plants and cyanobacteria are due to the generation of reactive oxygen species, which affects both the reduced and the oxidized sites of PSII (Al-Taweel et al. 2007; Takahashi and Murata 2008). Allakhverdiev et al. (2000) reported that, in addition to PSII, PSI is equally

inactivated by osmotic stress—the present study is focused on further exploring the role of PSI damage in salt stress.

In eukaryotes, the light-harvesting capacity of PSI and PSII is augmented by the membrane-intrinsic light harvesting complexes LHCI and LHCII. The LHCI proteins are associated only with PSI and deliver excitation energy to the PSI core. To the best of our knowledge, there have been no studies on the effects of salt stress on PSI-LHCI supercomplexes. We have used *C. reinhardtii* as a model system to study the effects of high salt conditions on PSI-LHCI supercomplexes. The present study focuses on changes in the protein profile of PSI-LHCI supercomplexes as well as the processes of energy transfer and trapping.

Materials and methods

Isolation of PSI-LHCI supercomplexes

Chlamydomonas reinhardtii cells (obtained from the *Chlamydomonas* culture collection at Duke University) were grown following standard procedures (Subramanyam et al. 2006). Cells were grown under both control (NaCl-free) and salt stress (100 mM NaCl) conditions with continuous illumination ($30–40$ μmol m^{-2} s^{-1}) to a density where $OD_{650nm} \sim 1$. Cells were then lysed and thylakoid membranes isolated according to Fischer et al. (1997) and resuspended in 200 mM sorbitol, 5 mM Tris–HCl (pH 8.0), 5 mM $CaCl_2$. PSI-LHCI supercomplexes were isolated as previously described (Kargul et al. 2003; Subramanyam et al. 2006). Following sucrose density gradient centrifugation, the lowest band was collected and diluted with three volumes of 5 mM Tris–HCl pH 8.0, 0.05% DDM, 5 mM $CaCl_2$. The diluted samples were then concentrated using a Centricon 100 ultrafiltration device (Amicon, Beverly, MA, USA) at 4,000 g in a Sorvall SS-34 rotor at 4°C.

Oxygen uptake and SOD activity measurements

PSI-mediated electron transfer from reduced dichlorophenol indophenol ($DCIPH_2$) to methyl viologen (MV) was measured by light-induced O_2 consumption using a Hansatech oxygen electrode at 22°C. White light illumination (250 W m^{-2}) was provided by a 150-W quartz-halogen projector lamp. The reaction mixture was composed of PSI-LHCI supercomplexes (15 mg Chl/ml), 20 mM Tricine-KOH (pH 8), 200 mM MV, 1 mM NaN_2, 100 mM $DCIPH_2$, 5 mM ascorbate, and 10 mM 3-(3,4 dichlorophenyl)-1,1-dimethylurea (DCMU). Samples were incubated in the dark for 5 min before measuring.

For superoxide dismutase (SOD) activity measurements, thylakoid membranes were suspended in 10 mM Tris–HCl (pH 7.5), 0.3 M sorbitol, 1.5 m M $CaCl_2$, 10 mM $MgCl_2$,

and activity was assayed according to Beauchamp and Fridovich (1971). The required cocktail for SOD activity estimation was prepared by mixing 27 ml of 50 mM sodium phosphate buffer (pH 7.8), 1.5 ml of methionine (300 mg ml^{-1}), 1 ml of NBT (14.4 mg 10 ml^{-1}), 0.75 ml of Triton X 100 and 1.5 ml of EDTA. 10 µl of riboflavin (4.4 mg 100 ml^{-1}) and 50 µg of protein were then added to this mixture. After the contents were mixed in a cuvette, they were illuminated for 12 min using a Comptalux bulb (Philips, Eindhoven, The Netherlands) and the absorbance was measured at 560 nm.

SDS-denaturing gel electrophoresis and in-gel trypsin digestion

For the analysis of the protein composition of PSI-LHCI supercomplexes from *C. reinhardtii,* samples were size-fractionated by gradient SDS-PAGE (15–23%). Equal amounts of protein (100 µg) were loaded on each lane. The PSI-LHCI supercomplexes were solubilized in 2% SDS and 0.1 M dithiothreitol, and the gel was stained with Coomassie brilliant blue R250. The desired bands were excised and diced into 1 mm^3 fragments, and then washed three times with 400 µl 50% acetonitrile, 50 mM Tris–HCl, pH 8.0, for 15 min to remove the Coomassie blue dye. Gel fragments were then soaked in 100% acetonitrile for 5 min, acetonitrile was removed and the sample was dried in a SpeedVac for 20 min at room temperature. Dried gel slices were rehydrated in 40 µl of 50 mM Tris–HCl, pH 8.0, containing 400 ng of porcine trypsin (Princeton separations, sequencing grade). The samples were digested for 18 h at 37°C, extracted with 50% acetonitrile, 5% trifluoroacetic acid for 30 min, and dried on a SpeedVac.

MALDI-TOF mass spectrometry and database searches

Tryptic peptides were desalted using C18 ZipTips (Millipore, Billerica, MA, USA) and eluted with 10 µl of 50% acetonitrile, 0.1% trifluoroacetic acid. 2 µl aliquots of the sample were mixed with 1.5 µl of matrix (a saturated solution of α-cyano-4-hydroxycinnamic acid in 50% acetonitrile, 0.1% trifluoroacetic acid) and a droplet of the mixture (about 1.5 µl) was spotted on the sample plate and dried. Mass spectra were collected on an Applied Biosystems Voyager DE-STR mass spectrometer (Applied Biosystems, Foster City, CA, USA) and analyzed with Data Explorer software. From the monoisotopic masses obtained, the amino acid sequences of matching tryptic fragments of *C. reinhardtii* PSI-LHCI proteins were obtained using the MS-Fit program of the online Protein Prospector software package (University of California, San Francisco, CA, USA) and the ExPASy Proteomics Server, as previously reported (Subramanyam et al. 2006).

Immunoblot analysis

PSI-LHCI polypeptides were separated by polyacrylamide gel electrophoresis (PAGE). Electrophoresis was performed on a 15% separating and 4% stacking gel of polyacrylamide. Equal quantities of protein were loaded onto each lane. An equal volume of 2× buffer was added to the aliquots. To identify and quantify the polypeptides contained in the PSI-LHCI supercomplex, immunoblotting was carried out essentially as described by Towbin et al. (1979). Immunoblotting was performed by electrophoretic transfer of proteins to PVDF membranes. The membrane was incubated with polyclonal antibodies raised in rabbits. We have used the specific primary antibodies against PsaB, PsaC, PsaE and PsaF. PsaB and PsaC were purchased from Agrisera (Vännäs, Sweden) and PsaE and PsaF antibodies were a gift from Prof. Kevin Redding (Arizona State University, USA). Subsequently, secondary antibodies ligated to horseradish peroxidase were applied. Chemiluminescence reagents were used to develop the PVDF membrane. The images were recorded on a Bio-Rad CCD camera.

Circular dichroism measurements

Visible circular dichroism spectra were measured in a J-810 spectropolarimeter (Jasco Inc., Easton, MD, USA). The optical path length of the cell was 1 cm, and the distance of the sample from the photomultiplier was 5 cm. The spectra were recorded in 1 nm steps with an integration time of 0.3 s and a band pass of 2 nm.

Ultrafast fluorescence spectroscopy

The time versus wavelength fluorescence intensity surfaces were recorded on a system consisting of an ultrafast laser and a streak camera, as described previously (Lidell et al. 2008). Briefly, 130 fs light pulses at 800 nm were generated by a mode-locked Ti:S laser (Mira 900, Coherent Laser Inc., Santa Clara, CA, USA) pumped by a frequency-doubled Nd:YVO$_4$ laser (44% from an 18 W Verdi, Coherent Laser Inc.). The repetition rate of the Ti:S laser was reduced to 4.75 MHz by a pulse picker (Model 9200, Coherent Laser Inc.). The excitation light (800 nm) was frequency doubled to 400 nm and focused onto a sample cuvette with a 5 mm path length. Fluorescence was collected at a right angle to the excitation beam and focused on the entrance slit of a Chromex 250IS spectrograph which was coupled to a Hamamatsu C5680 streak camera with a M5675 synchroscan sweep unit. The streak images were recorded on a Hamamatsu C4742 CCD camera. Measurements were performed on 800 ps, 1.4, and 2 ns timescales, with 1,024 pixels of time resolution. The FWHM of the overall time response of this system was ∼6 ps at the

800 ps timescale, ~12 ps at the 1.4 ns timescale, and ~20 ps at the 2 ns timescale. The spectral resolution was 0.124 nm in the spectral range of 650–777 nm (1,024 pixels). To avoid singlet–singlet annihilation, the pulse energy was reduced to 0.1 nJ using a neutral density filter. The probability of a single supercomplex absorbing multiple photons in a single laser pulse was estimated using Poisson statistics (Cho et al. 1984) and it was found that less than 2% of emitted photons could have come from supercomplexes which had received multiple excitations. Global analysis was performed using locally written software in MATLAB. The 1,024 kinetic traces were binned, resulting in a spectral resolution of 1.24 nm. A Gaussian shaped instrument response function was used in the fitting.

Results

Trial experiments were carried out to determine a suitable concentration of NaCl to use for salt-stress studies of *C. reinhardtii*. The cells were grown with NaCl concentrations ranging from 10 to 1,000 mM. Cells could not be grown at concentrations greater than 150 mM; 100 mM concentration was used for stress conditions in this study. Both control and salt-stressed cells were grown to ~1 OD at 650 nm. A delay in growth was observed in medium with 100 mM NaCl (data not shown).

Sucrose gradient analysis

PSI-LHCI supercomplexes were isolated using sucrose density gradient centrifugation. The detergent extracts of the thylakoid membranes were loaded onto the gradient at equal Chl levels (0.8 mg/ml Chl). After the centrifugation, three distinct bands were observed in both the control and the salt stress samples; the fractions corresponded to F1 (LHCII), F2 (PSI-LHCI and PSII) and F3 (PSI-LHCI supercomplexes), as shown in our previous report (Subramanyam et al. 2006) (Fig. 1). For this study, PSI-LHCI supercomplexes (F3) were collected from the sucrose gradient. No significant difference in the bands was observed between the control and salt stress samples (see Fig. 1).

Oxygen uptake analysis and antioxidant enzyme analysis

The electron transfer activity of purified PSI-LHCI supercomplexes from *C. reinhardtii* cells grown at 50 and 100 mM NaCl was measured by assaying O_2 uptake, as described above. PSI activity was reduced by 18 and 39%, respectively (Fig. 2a) compared to the control sample. This result indicates that the activity of the reducing side of PSI

Fig. 1 Separation of PSI-LHCI supercomplexes from solubilized thylakoid membranes by sucrose density centrifugation. F1 (LHCII), F2 (PSI-LHCI and PSII) and F3 (PSI-LHCI supercomplexes). See "Materials and methods" for further details
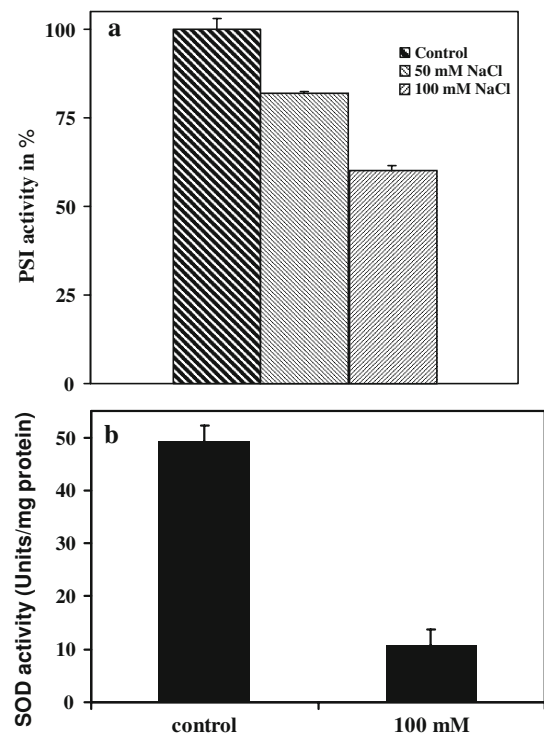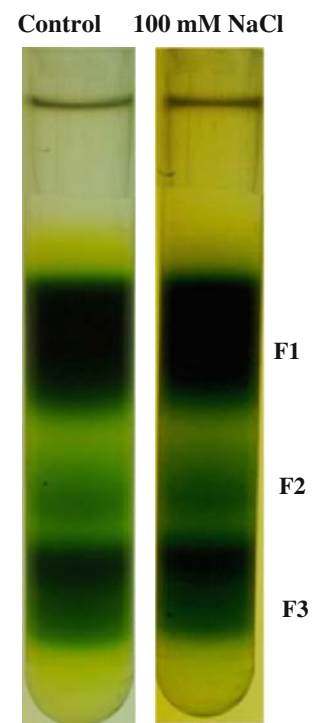
Fig. 2 a O_2-uptake activity of PSI-LHCI supercomplexes isolated from cells grown at 0 (control), 50, and 100 mM NaCl. The PSI activity is 350 μmol mg^{-1} Chl h^{-1}. **b** Total SOD activity

is reduced under salt stress. Total SOD activity was decreased by 78% in thylakoids isolated from cells grown at 100 mM, relative to cells grown under control conditions (Fig. 2b).
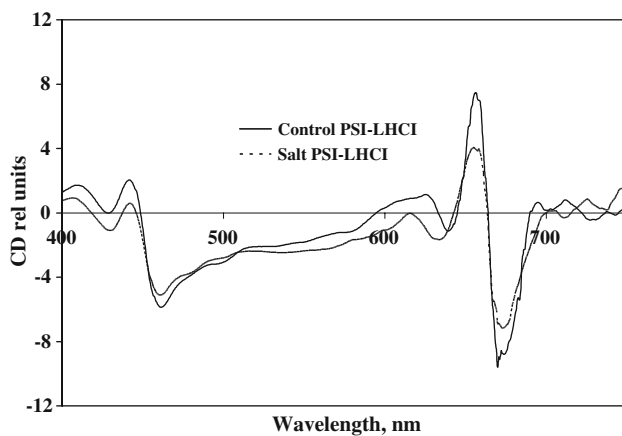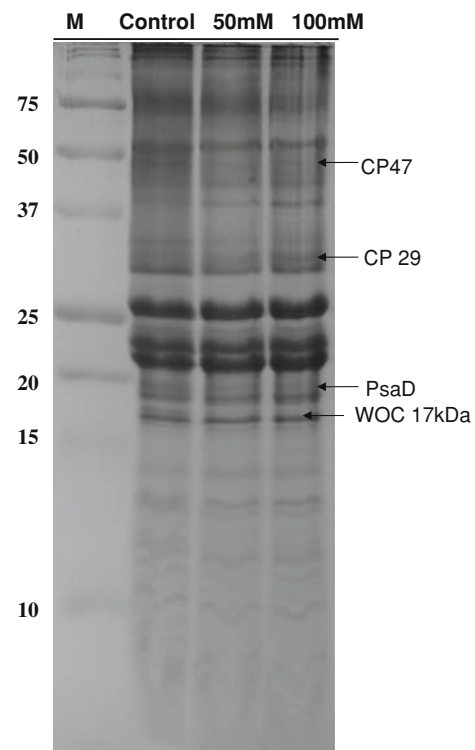
Visible CD data analysis

Visible CD spectroscopy is a sensitive monitor of excitonic pigment–pigment interactions and pigment–protein interactions. In the Q_y region, there are two negative peaks at 640 and 672 nm and one positive peak at 656 nm (Fig. 3), similar to our previous report (Subramanyam et al. 2006). The two major bands at 656 and 672 nm are due to Chl dimers caused by the excitonic interaction of Chl *a* in PSI–LHCI supercomplexes, while the negative peak at 640 nm is characteristic of Chl *b* (Bassi and Simpson 1987; Subramanyam et al. 2006). In the Soret region, the positive peak at 443 nm originates from Chl *a*, while the negative peak at 460 nm is characteristic of Chl *b*. The visible CD spectrum of PSI-LHCI supercomplexes isolated from *C. reinhardtii* cells grown at high salt (100 mM) shows a decrease in the amplitude of the major peaks at 656 and 672 nm. The negative peak at 642 nm showed an increase in amplitude relative to the control, along with a blue shift of about 7 nm. The Soret band peaks at 443 and 460 nm also decreased in intensity. The differences in the peak intensity indicate significant differences in pigment interactions in PSI-LHCI complexes from salt stressed cells.

Effect of salt stress on the protein content of PSI-LHCI supercomplexes

The proteins were separated by SDS-gel electrophoresis and individual proteins identified by MALDI-TOF mass spectrometry and immunoblotting. Figures 4 and 5 show that there is no change in content of the reaction center core proteins PsaA and PsaB. Thylakoids isolated from cells grown at different NaCl concentrations (0, 50, and 100 mM) show that several proteins, including components of PSII and PSI, were affected (Fig. 4). It appears that, under the experimental conditions used, both PSII and PSI
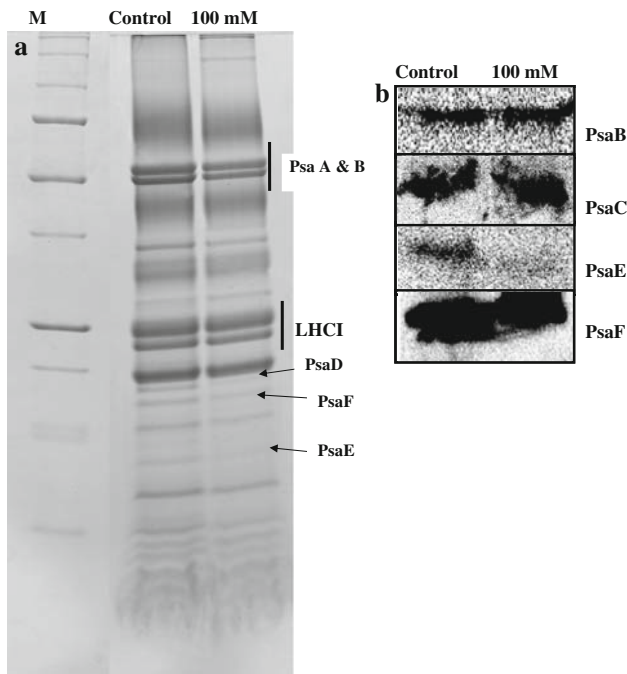

Fig. 4 Comparison of the SDS–PAGE polypeptide profiles of thylakoids from *C. reinhardtii* cells grown under control and salt-stress conditions. A 15–23% gradient gel was used for SDS-PAGE. Equal amounts of protein (100 μg) were loaded onto each lane

Fig. 3 Visible CD spectra of isolated PSI–LHCI supercomplexes from control and salt-stressed *C. reinhardtii* cells. The Chl content of the samples was adjusted to 10 μg/ml. CD was measured in absorbance units. However, for easier comparison, the data are plotted in relative units. Experimental conditions are given in "Materials and methods"

are down regulated by salt stress. Surprisingly, levels of the Lhca proteins remain unchanged (Fig. 5a), suggesting that the important changes in antenna function may come from disruption of pigment binding to proteins or disruption of the PSI-LHCI interface, rather than from reduced Lhca protein synthesis. More importantly, levels of the PsaD, PsaF, and PsaE proteins were reduced (Fig. 5a). The content of PsaD is decreased upon increasing concentration of NaCl; the PsaD band is clearly visible in the control thylakoids (see Fig. 4). This band has been identified as PsaD by MALDI-TOF. The monoisotopic masses obtained from MALDI-TOF were analyzed using the Aldente peptide mass fingerprinting tool (http://www.expasy.org/tools/aldente/) (Tuloup et al. 2003) and a match was found to PsaD from *C. reinhardtii* in thylakoids. Of all the PSI subunits, PsaE seems to be the most sensitive and is completely depleted by salt stress (Fig. 5b). The immunoblot data also confirm that levels of these subunits were reduced due to salt stress. In contrast to the other membrane-extrinsic subunits, levels of PsaC did not change.

Streak camera data analysis

Fluorescence decay spectra were measured using an ultrafast streak camera setup for PSI-LHCI supercomplexes

Fig. 5 **a** Comparison of the SDS-PAGE polypeptide profiles of PSI-LHCI supercomplexes from *C. reinhardtii* cells grown under control and salt-stress conditions. A 15–23% gradient gel was used for SDS-PAGE. Equal amounts of protein (100 µg) were loaded onto each lane. PsaD, PsaF and PsaE were identified by MALDI-TOF. **b** Quantitative immunoblot analysis of PSI-LHCI supercomplexes from isolated from control (NaCl-free) and salt-stress (100 mM NaCl) cells. All experimental conditions are given in "Materials and methods"

Table 1 Trapping lifetimes obtained from streak camera measurements

| Sample	τ_1 (ps)	τ_2
Control	32.1 ± 3.6	172.26 ± 42.4
NaCl stress	31.6 ± 3.8	156.5 ± 32.8
Timescale		
800 ps	29.8 ± 3.4	136.1 ± 23.6
1.4 ns	33.4 ± 2.4	161.1 ± 13.2
2 ns	34.9 ± 1.7	196.5 ± 21.2

Only the lifetimes of the first two components are presented; the third was typically fixed at 4 ns during fitting and does not represent functional antenna pigments. Values are mean ± SE ($n = 8$)

isolated under salt stress, and for control conditions. For each sample, kinetics were measured on 800 ps, 1.4, and 2 ns timescales and fit to three decay components.

The component with the shortest lifetime was very consistent across samples and timescales, with a lifetime of ~33 ps. Based on comparison with previous studies of excitation trapping in PSI (Gobets and van Grondelle 2001), this component of the fluorescence decay can be attributed to the trapping of excitons originating within the PSI core. The second component, which has previously been associated with the trapping of excitons originating in the peripheral LHCI complexes (Ihalainen et al. 2005), is more heterogeneous. As is shown in Table 1, however, the variations between samples measured at different time scales are more significant than the differences between the three samples. Although fitting the fluorescence decay with three exponentials provides a convenient description of the kinetics, it must be kept in mind that the real process being measured is far more complicated—the lifetimes found by global analysis merely provide characteristic time scales for various decay processes. Variation of the lifetime found by global analysis with measurement timescale can be attributed to heterogeneity within this decay phase.

Far more insight into the nature of these decay phases can be obtained by examining the spectral shapes of the three decay components. The shape of the first (~33 ps) component is extremely consistent among the samples measured (Fig. 6a). Given that the PsaA and PsaB proteins, which bind the bulk of PSI's core antenna, appear based on immunoblotting results to be largely unaffected by salt stress, this suggests strongly that only pigments bound to the PSI core contribute to this component. This is consistent with structural studies (Jordan et al. 2001; Amunts et al. 2007) that show that the PSI core is a stable, tightly integrated complex. Similar conservation can be seen in the spectral shapes of the third component (3–4 ns); such lifetimes are typically attributed to detergent-solubilized Chl that is not coupled to PSI (Fig. 6c). It should be noted that the amplitude of the nanosecond component was much lower in the control sample than in the stress samples and the spectral shapes could only be compared after normalization. This indicates that the PSI-LHCI from salt stressed cells contains more uncoupled pigments.

The major difference in the decay-associated spectra of the control and salt-stress samples can be seen in the spectral shape of the 120–220 ps component (Fig. 6b). While the decay lifetimes are relatively unchanged by cell growth under salt stress conditions, this component shows a decrease in emission intensity on the red side of the peak in the salt-stressed samples. Red emission in *C. reinhardtii* PSI has previously been associated with strongly coupled pigments bound by the LHCI proteins (Gibasiewicz et al. 2001, 2002, 2005) and so this loss of red emission can be attributed to a disruption of the LHCI antenna system.

Discussion

The primary objective of this work was to evaluate the effects of salt stress on PSI-LHCI supercomplexes from *C. reinhardtii*, in an effort to understand the effects of stress on PSI function. Previous research has shown that many
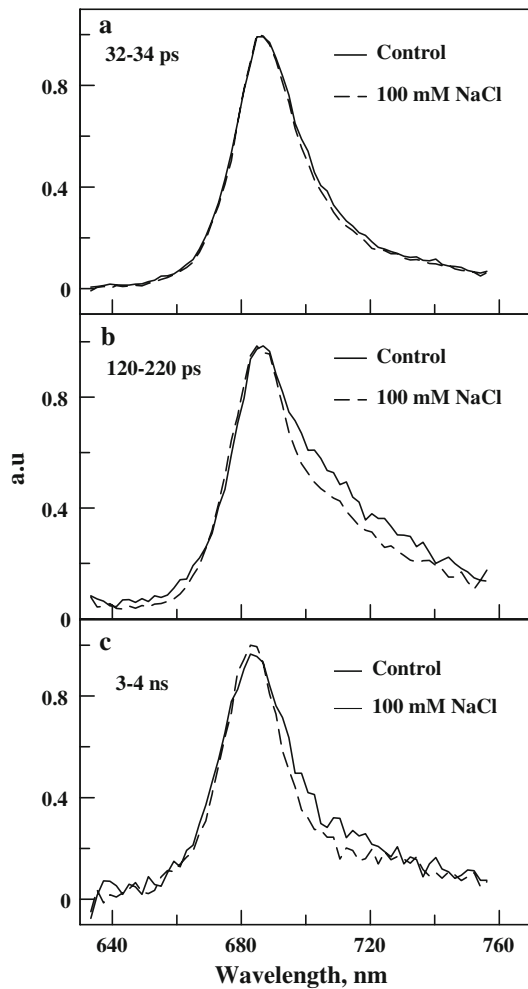
Fig. 6 Representative fluorescence decay-associated spectra (FDAS) obtained from fluorescence streak camera measurements from isolated PSI-LHCI supercomplexes obtained from *C. reinhardtii* grown under control (NaCl-free) and stress (100 mM NaCl) conditions. Fluorescence decay lifetimes are 35–38 ps (**a**), 22–211 ps (**b**), and 2–4 ns (**c**). Each curve shown is the average of the fitted curves from the three data sets collected for each sample

types of abiotic stress affect PSII, but the extent of damage for PSI is less well studied. Our results indicate that stress-related damage to PSI is also significant and may be an important part of the organism's overall stress response.

C. reinhardtii cells were grown at NaCl concentrations of 0 (control) and 100 mM, reaching an OD of ~1 at 650 nm. The control cells reached this growth within four days; growth in high-salt medium took 5 days to reach the same density. High salt conditions clearly impair cell growth; the goal of this study has been to establish the degree to which this growth impairment results from damage to PSI-LHCI. In particular, we have attempted to determine the structural integrity of PSI-LHCI under salt stress, as well as functional changes associated with structural rearrangements. The electron transfer activity was decreased (Fig. 2a), but levels of the subunits PsaA and

PsaB, which form the core of PSI and bind the majority of the cofactors of the electron transfer chain (ETC) (P700, A, A_O, phylloquinones (A_1) and the 4Fe4S clusters, F_X) (ETC), were unchanged. This suggests that the impairment may lie in energy transfer from LHCI to PSI core, or in damage to the acceptor side of PSI (terminal FeS clusters $F_A + F_B$), rather than to the oxidizing side of the ETC.

In keeping with these results, the fluorescence decay component associated with trapping in the PSI core was virtually unchanged between the control and salt stress samples (Fig. 6a). The 32–34 ps compound arises from PSI core (Gobets and van Grondelle 2001) in our results but there is no difference in fluorescence lifetime in the control and salt stress samples (Fig. 6a) indicating that the PSI core antenna is not affected. Differences were quite apparent in the second component (Fig. 6b), which decays on the 120–220 ps timescale. The curves look similar on the blue side of the emission peak, but the stressed samples show significantly less emission on the red side than the control sample. Red-shifted pigments in photosynthetic systems typically arise from strongly coupled dimers of Chl molecules and may exert a significant influence on the exciton trapping dynamics. Previous spectroscopic studies of green algal PSI (Gibasiewicz et al. 2001, 2002, 2005) have indicated that the PSI core in *C. reinhardtii* does not contain any pigments with transition energies lower than that of P700— longer-wavelength pigments are associated only with the peripheral LHCI complexes. The loss of red-shifted emission in the salt samples can therefore be attributed to the change in pigment–pigment interactions of LHCI complexes under stress conditions. The disruption of the red sites probably results from an overall decrease in the quality of PSI-LHCI coupling, which would cause more energy to be lost as fluorescence rather than being delivered to the core. In general, partially disrupted LHCI proteins would lead to the formation of more chlorophyll triplet states and would get oxidative damage to the core but in salt stress the damage was due to ROS production. Thus, in salt stress it may be different excitation energy distribution from LHCI to PSI core.

The visible CD data show an increase in amplitude at 676 and 656 nm, which can be attributed to a loss of tightly coupled Chl *a* in the LHCI antenna. The peak associated with Chl *b* shifts from 640 to 630 nm under salt stress conditions (Fig. 3), suggesting a change in pigment–pigment interactions and may arise, for example, from a change of the Chl *a*–Chl *b* distance.

The stromal acceptor side of the PSI reaction center is damaged by high salt conditions. Our results show (Figs. 4, 5) a clear reduction in the membrane-extrinsic PsaD and PsaE subunits, as well as the transmembrane PsaF subunit of PSI. The reduction is most dramatic in the case of PsaE in both thylakoids and isolated PSI-LHCI supercomplexes.

The crystal structure of *Thermosynechococcus* PSI shows that PsaE stabilizes the stromal hump and the interaction between the PsaA/B heterodimer and PsaC (Jordan et al. 2001; Jensen et al. 2007). The higher plant PSI structure retains the same organization as the cyanobacterial complex (Amunts et al. 2007); we assume that green algal PSI also retains the same overall architecture. From our data, it is clear that the degradation of the PSI stromal ridge begins at PsaE and PsaD. The PsaE protein is located at the reducing side of photosystem I (PSI) and stabilizes the stromal hump that is involved in docking the soluble electron acceptors, particularly ferredoxin/flavodoxin (Lelong et al. 1996; Jordan et al. 2001; Jensen et al. 2007). While PsaC binds the terminal electron acceptors F_A and F_B and is essential for the function of PSI (Oh-Oka et al. 1988), PsaD and PsaE stabilize PsaC and the stromal hump that is involved in ferredoxin binding (Chitnis et al. 1995; Sétif et al. 2002).

The damage to PSI subunits is associated with a decrease in SOD activity; this decrease probably results in higher levels of reactive oxygen species. Similar results have been observed in Cd stress in plants (Somashekaraiah et al. 1992; Chaoui et al. 1997; Sandalio et al. 2001). The loss of PsaE at the reducing side of PSI may cause electron leakage to oxygen in the light (Mehler reaction), resulting in the formation of reactive oxygen species which could in turn damage the Fe–S clusters. These results agree with a very recent report of a deletion mutant of *psaE* in the cyanobacterium *Synechocystis sp.* strain PCC 6803, which shows increased photodamage due to formation of oxygen radicals (Jeanjean et al. 2008). As a result, the ferredoxin-docking site near the stromal Fe–S clusters is destabilized, crippling electron transfer through PSI.

Mutagenesis studies have indicated that the subunits on the reducing side of PSI assemble in a well-defined order: PsaC first, followed by PsaD and PsaE (Yu et al. 1995; Zhao et al. 1993). Under salt-stress conditions, the decrease in levels of PsaD (Fig. 4) results in the near-elimination of PsaE (Fig. 5b); this correlation supports a scheme in which the presence of PsaD is a prerequisite for PsaE binding (Lüneberg et al. 1994). Immunoblotting results also indicate that the levels of PsaC are virtually unchanged under salt stress (Fig. 5b); this is consistent with an assembly pathway in which PsaC binds first (Jolley et al. 2006) and is removed last when the complex is disassembled. This likely does not mean, however, that the function of PsaC is unimpacted by salt stress; PsaD has been proposed to play a role in the structural stabilization of the otherwise labile PsaC (Li et al. 1991; Chitnis et al. 1996), and the magnetic properties of the terminal FeS clusters F_A and F_B, which bind to PsaC, are affected by the presence of PsaD (Golbeck 1999; Vassiliev et al. 2001). In summary, these results indicate that the acceptor side of PSI is strongly affected by salt

stress and the electron transfer capabilities of F_A and F_B could be severely impacted, even if levels of PsaC are unchanged. Furthermore, it is known that the LHCI proteins attach to PSI near PsaF (Ben-Shem et al. 2003; Amunts et al. 2007), so the decrease of PsaF under salt stress could explain the loss of LHCI-associated red emission observed in the fluorescence decay-associated spectra (Fig. 6). All of these results appear to be triggered by the accumulation of ROS damage in the absence of effective protection from SOD; this supports the idea that accumulation of SOD in response to salt, drought and cold stress plays a crucial role in helping the cell to survive under environmental stress conditions.

SOD is influencing the changes in PSI organization. However, PSII was also damaged and thus the *C. reinhardtii* cell growth was impaired due to the change in both PSII and PSI.

References

Allakhverdiev SI, Murata N (2008) Salt stress inhibits photosystems II and I in cyanobacteria. Photosynth Res 98:529–539

Allakhverdiev SI, Nishiyama Y, Suzuki I, Tasaka Y, Murata N (1999) Genetic engineering of the unsaturation of fatty acids in membrane lipids alters the tolerance of *Synechocystis* to salt stress. Proc Natl Acad Sci USA 96:5862–5867

Allakhverdiev SI, Sakamoto A, Nishiyama Y, Inaba M, Murata N (2000) NaCl-induced inactivation of photosystems I and II in *Synechococcus*: osmotic effects and ionic effects. Plant Physiol 123:1047–1056

Al-Taweel K, Iwaki T, Yabuta Y, Shigeoka S, Murata N, Wadano A (2007) A bacterial transgene for catalase protects translation of D1 protein during exposure of salt-stressed tobacco leaves to strong light. Plant Physiol 145:258–265

Amunts A, Drory O, Nelson N (2007) The structure of a plant photosystem I supercomplex at 3.4 Å resolution. Nature 44:58–63

Bassi R, Simpson D (1987) Chlorophyll–protein complexes of barley photosystem I. Eur J Biochem 163:221–230

Beauchamp CO, Fridovich I (1971) Superoxide dismutase: improved assays and an assay applicable to acrylamide gels. Anal Biochem 44:276–287

Ben-Shem A, Frolow F, Nelson N (2003) Crystal structure of plant photosystem I. Nature 426:630–635

Brini FB, Hanin M, Mezghani I, Berkowitz GA, Masmoudi K (2007) Overexpression of wheat Na+/H+ antiporter TNHX1 and H+-pyrophosphatase TVP1 improve salt- and drought-stress tolerance in *Arabidopsis thaliana* plants. J Exp Bot 58:301–308

Chaoui A, Mazhoudi S, Ghorbal MH, El Ferjani E (1997) Cadmium and zinc induction of lipid peroxidation and effects on antioxidant enzymes activities in bean (*Phaseolus vulgaries* L.). Plant Sci 127:139–147

Chitnis PR, Xu Q, Chitnis VP, Nechushtai R (1995) Function and organization of photosystem I polypeptides. Photosynth Res 44:23–40

Chitnis VP, Jungs YS, Albee L, Golbeck JH, Chitnis PR (1996) Mutational analysis of photosystem I polypeptides. Role of PsaD and the lysyl 106 residue in the reductase activity of the photosystem I. J Biol Chem 271:11772–11780

Cho HM, Mancino LJ, Blankenship RE (1984) Light saturation curves and quantum yields in reaction centers from photosynthetic bacteria. Biophys J 45:455–4613

Demetriou G, Neonaki C, Navakoudis E, Kotzabasis K (2007) Salt stress impact on the molecular structure and function of the photosynthetic apparatus—the protective role of polyamines. Biochim Biophys Acta 1767:272–280

Endo T, Schreiber U, Asada K (1995) Suppression of quantum yield of photosystem II by hyperosmotic stress in *Chlamydomonas reinhardtii*. Plant Cell Physiol 36:1253–1258

Everard JD, Gucci R, Kann SC, Flore JA, Loescher WH (1994) Gas exchange and carbon partitioning in the leaves of celery (*Apium graveolens* L.) at various levels of root zone salinity. Plant Physiol 106:281–292

Fischer N, Setif P, Rochaix JD (1997) Targeted mutations in the psaC gene of *Chlamydomonas reinhardtii*: preferential reduction of FB at low temperature is not accompanied by altered electron flow from photosystem I to ferredoxin. Biochemistry 36:93–102

Gibasiewicz K, Ramesh VM, Melkozernov AN, Lin S, Woodbury NW, Blankenship RE, Webber AN (2001) Excitation dynamics in the core antenna of PS I from *Chlamydomonas reinhardtii* CC 2696 at room temperature. J Phys Chem B 105:11498–11506

Gibasiewicz K, Ramesh VM, Lin S, Woodbury NW, Webber AN (2002) Excitation dynamics in eukaryotic PS I from *Chlamydomonas reinhardtii* CC 2696 at 10 K. Direct detection of the reaction center exciton states. J Phys Chem B 106:6322–6330

Gibasiewicz K, Szrajner A, Ihalainen JA, Germano M, Dekker JP, van Grondelle R (2005) Characterization of low-energy chlorophylls in the PSI-LHCI supercomplex from *Chlamydomonas reinhardtii*. A site-selective fluorescence study. J Phys Chem B 109:21180–21186

Gilmour DJ, Hipkins MF, Webber AN, Baker NR, Boney AD (1985) The effect of ionic stress on photosynthesis in *Dunaliella tertiolecta*. Chlorophyll fluorescence kinetics and spectral characteristics. Planta 163:250–256

Gobets B, van Grondelle R (2001) Energy transfer and trapping in photosystem I. Biochim Biophys Acta 1507:80–99

Golbeck JH (1999) A comparative analysis of the spin state distribution of in vitro and in vivo mutants of PsaC. A biochemical argument for the sequence of electron transfer in photosystem I as $F_X \rightarrow F_A \rightarrow F_B \rightarrow$ ferredoxin/flavodoxin. Photosynth Res 61:107–144

Gong H, Tang Y, Wang J, Wen X, Zhang L, Lu C (2008) Characterization of photosystem II in salt-stressed cyanobacterial *Spirulina platensis* cells. Biochim Biophys Acta 1777:488–495

Ihalainen JA, Klimmek F, Ganeteg U, van Stokkum IH, van Grondelle R, Jansson S, Dekker JP (2005) Excitation energy trapping in photosystem I complexes depleted in Lhca1 and Lhca4. FEBS Lett 579:4787–4791

Jeanjean R, Latifi A, Matthijs HCP, Havaux M (2008) The PsaE subunit of photosystem I prevents light-induced formation of reduced oxygen species in the cyanobacterium *Synechocystis* sp. PCC 6803. Biochim Biophys Acta 1777:308–316

Jensen PE, Bassi R, Boekema EJ, Dekker JP, Jansson S, Leister D, Robinson C, Scheller HV (2007) Structure, function and regulation of plant photosystem I. Biochim Biophys Acta 1767:335–352

Jolley CC, Wells SA, Hespenheide BM, Thorpe MF, Fromme P (2006) Docking of photosystem I subunit C using a constrained geometric simulation. J Am Chem Soc 128:8803–8812

Jordan P, Fromme P, Witt HT, Klukas O, Saenger W, Krauss N (2001) Three-dimensional structure of cyanobacterial photosystem I at 2.5 Å resolution. Nature 411:909–917

Kargul J, Nield J, Barber J (2003) Three-dimensional reconstruction of a light-harvesting complex I–photosystem I (LHCI-PSI) supercomplex from the green alga *Chlamydomonas reinhardtii*. Insights into light harvesting for PSI. J Biol Chem 278:16135–16141

Lelong C, Boekema EJ, Kruip J, Bottin H, Rögner M, Sétif P (1996) Characterization of a redox active cross-linked complex between cyanobacterial photosystem I and soluble ferredoxine. EMBO J 15:2160–2168

Li N, Zhao JD, Warren PV, Warden JT, Bryant DA, Golbeck JH (1991) PsaD is required for the stable binding of PsaC to the photosystem I core protein of *Synechococcus* sp. PCC 6301. Biochemistry 30:7863–7872

Lidell PA, Gervaldo M, Bridgewater JW, Keirstead AE, Lin S, Moore TA, Moore AL, Gust D (2008) Porphyrin-based hole conducting electropolymer. Chem Mater 20:135–142

Lu C, Vonshak A (1999) Characterization of PSII photochemistry in salt-adapted cells of cyanobacterium *Spirulina platensis*. New Phytol 141:231–239

Lu C, Vonshak A (2002) Effects of salinity on photosystem II function in cyanobacterial *Spirulina platensis* cells. Physiol Plant 114:405–413

Lüneberg J, Fromme P, Jekowa P, Schlodde E (1994) Spectroscopic characterization of PSI core complexes from thermophilic *Synechococcus* sp: Identical reoxidation kinetics of A^{-1} before and after removal of the iron-sulfur-clusters F_A and F_B. FEBS Lett 338:197–202

Misra AN, Sahu SM, Mishra M, Ramaswamy NK, Desai TS (1999) Sodium chloride salt stress induced changes in thylakoid pigment-protein complexes, photosystem II activity and thermoluminescence glow peaks. Z Naturforsch 54c:640–644

Miyao M, Murata N (1983) Partial disintegration and reconstitution of the photosynthetic oxygen–evolution system: binding of 24 kDa and 18 kDa polypeptides. Biochim Biophys Acta 725:87–93

Murata N, Miyao M (1985) Extrinsic membrane proteins in the photosynthetic oxygen-evolving complex. Trends Biochem Sci 10:122–124

Murata N, Mohanty PS, Hayashi H, Papageorgiou GC (1992) Glycinebetaine stabilizes the association of extrinsic proteins with the photosynthetic oxygen evolving complex. FEBS Lett 296:187–189

Oh-Oka H, Takahashi Y, Kuriyama K, Saeki K, Matsubara H (1988) The protein responsible for center A/B in spinach photosystem I: isolation with iron–sulfur cluster(s) and complete sequence analysis. J Biochem 103:962–968

Parida AK, Das AB, Mittra B (2003) Effects of NaCl stress on the structure, pigment complex composition, and photosynthetic activity of mangrove *Bruguiera parviflora* chloroplasts. Photosynthetica 41:191–200

Sandalio LM, Dalurzo HC, Gomez M, Romero-Puertas MC, del Rio LA (2001) Cadmium-induced changes in the growth and oxidative metabolism of pea plants. J Exp Bot 52:2115–2126

Satoh K, Smith CM, Fork DC (1983) Effects of salinity on primary processes of photosynthesis in the red alga *Porphyra perforata*. Plant Physiol 73:643–647

Sétif P, Fischer N, Lagoutte B, Bottin H, Rochaix J-D (2002) The ferredoxin docking site of photosystem I. Biochim Biophys Acta 1555:204–209

Somashekaraiah BV, Padmaja K, Prasad ARK (1992) Phytotoxicity of cadmium ions on germinating seedlings of mung bean (*Phaseolus vulgaries*): involvement of lipid peroxides in chlorophyll degradation. Physiol Plant 85:85–89

Subramanyam R, Jolley C, Brune DC, Fromme P, Webber AN (2006) Characterization of a novel photosystem I–LHCI supercomplex isolated from *Chlamydomonas reinhardtii* under anaerobic (state II) conditions. FEBS Lett 580:233–238

Sudhir P, Pogoryelov D, Kovács L, Garab G, Murthy SDS (2005) The effects of salt stress on photosynthetic electron transport and thylakoid membrane proteins in the cyanobacterium *Spirulina platensis*. J Biochem Mol Biol 38:481–485

Takahashi S, Murata N (2008) How do environmental stresses accelerate photoinhibition? Trends Plant Sci 13:178–182

Tiwari BS, Bose A, Ghosh B (1997) Photosynthesis in rice under a salt stress. Photosynthetica 34:303–306

Towbin H, Stahelin T, Gordon J (1979) Electrophoresis transfer of proteins from polyacrylamide gels to nitrocellulose sheets: procedure and some application. Proc Natl Acad Sci USA 76:43450–43454

Tuloup M, Hernandez C, Coro I, Hoogland C, Binz P-A, Appel RD (2003) Aldente and biograph: an improved peptide mass fingerprinting protein identification environment. In: Fontis Media (ed) Swiss Proteomics congress: understanding biological systems through proteomics. Basel, Switzerland, pp 174–176

Vassiliev IR, Antonkine ML, Golbeck JH (2001) Iron-sulfur clusters in type I reaction centers. Biochim Biophys Acta 1507:139–160

Verma K, Mohanty P (2000a) Changes of the photosynthetic apparatus in *Spirulina* cyanobacterium by sodium stress. Z Naturforsch 55c:16–22

Verma K, Mohanty P (2000b) Alterations in the structure of phycobilisomes of the cyanobacterium, *Spirulina platensis* in response to enhanced Na$^+$ level. World J Microbiol Biotechnol 16:795–798

Yu J, Smart LB, Jung YS, Golbeck J, McIntosh L (1995) Absence of PsaC subunit allows assembly of photosystem I core but prevents the binding of PsaD and PsaE in *Synechocystis sp*. PCC 6803. Plant Mol Biol 29:331–342

Zhao J, Snyder WB, Muhlenhoff U, Rhiel E, Warren PV, Golbeck JH, Bryant DA (1993) Cloning and characterization of the psaE gene of the cyanobacterium *Synechococcus* sp. PCC 7002: characterization of a psaE mutant and overproduction of the protein in *Escherichia coli*. Mol Microbiol 9:183–194